Bioorganic Chemistry 37 (2009) 41–45

Contents lists available at ScienceDirect

Bioorganic Chemistry

journal homepage: www.elsevier.com/locate/bioorg

Mapping of suramin binding sites on the group IIA human secreted phospholipase A_2

Davi Serradella Vieira [a], Elisangela Aparecida Aragão [a], Marcos Roberto Lourenzoni [b], Richard J. Ward [a,*]

[a] Departamento de Química, Faculdade de Filosofia, Ciências e Letras de Ribeirão Preto, Universidade de São Paulo, Avenida Bandeirantes 3900, Monte Alegre, CEP 14040-901, Ribeirão Preto-SP, Brazil
[b] Verdartis Desenvolvimento Biotecnológico Ltda ME, Campus USP, Ribeirão Preto, Brazil

ARTICLE INFO

Article history:
Received 20 October 2008
Available online 3 February 2009

Keywords:
Molecular dynamics
Isothermal titration calorimetry

ABSTRACT

Suramin is a polysulphonated napthylurea used as an antiprotozoal/anthelminitic drug, which also inhibits a broad range of enzymes. Suramin binding to recombinant human secreted group IIA phospholipase A_2 (hsPLA$_2$GIIA) was investigated by molecular dynamics simulations (MD) and isothermal titration calorimetry (ITC). MD indicated two possible bound suramin conformations mediated by hydrophobic and electrostatic interactions with amino-acids in three regions of the protein, namely the active-site and residues located in the N- and C-termini, respectively. All three binding sites are located on the phospholipid membrane recognition surface, suggesting that suramin may inhibit the enzyme, and indeed a 90% reduction in hydrolytic activity was observed in the presence of 100 nM suramin. These results correlated with ITC data, which demonstrated 2.7 suramin binding sites on the hsPLA$_2$GIIA, and indicates that suramin represents a novel class of phospholipase A_2 inhibitor.

1. Introduction

Phospholipases A_2 (PLA$_2$ – EC 3.1.1.4) catalyze the hydrolysis the *sn*-2 acyl bonds of *sn*-3 phospholipids [1], and on the basis of amino acid sequence similarity are classified in 15 groups [2]. The human secreted group IIA PLA$_2$ (hsPLA$_2$GIIA) is present in various secretions, including high concentrations in inflammatory fluids [3] and human tears [4], and is also expressed at significant levels in Paneth cells of the intestine [5] and macrophages [3,6]. The enzyme contains a high number of surface located positively charged amino acid residues (p*I* > 10.5), and demonstrates a high hydrolytic activity preferentially against both anionic vesicles and the plasma membranes of Gram-positive bacteria [7,8]. The current consensus is that the hydrolysis of membrane phospholipids by the hsPLA$_2$GIIA plays an important role in these biological activities.

Suramin is a polysulfonated napthylurea (see Fig. 1A) with a long history of clinical use as an anti-trypanossomal drug [9], which due to its highly anionic nature also binds to a wide range of basic proteins [10], including PLA$_2$s. It has been shown, for example, that suramin inhibits the neuromuscular blockade induced by neurotoxic PLA$_2$ isolated from snake venoms such as beta-bungarotoxin and crotoxin [11], and also inhibits the myotoxic and *in vitro* neuromuscular blocking activities of the cationic Lys49-PLA$_2$ from the venoms of viperid snake species [12]. Furthermore, we have recently demonstrated that suramin inhibits both the catalytic activity and macrophage activation by the secreted group IIA human PLA$_2$ (hsPLA$_2$GIIA), yet has no effect on the bactericidal effect of the protein against Gram-positive bacteria [13]. These studies demonstrate the potential of suramin to selectively inhibit the effects of the hsPLA$_2$GIIA against different cell types.

A wide variety of PLA$_2$ inhibitors have been reported that reduce the inflammatory effects of these enzymes [14,15]. In order to further understand the cell-type selectivity if the suramin inhibition against hsPLA$_2$GIIA, molecular dynamics simulations and isothermal titration calorimetry were used to investigate the thermodynamic parameters and the potential energy of the hsPLA$_2$-GIIA/suramin interaction with the aim of identifying the suramin binding sites on the protein.

2. Materials and methods

2.1. Chemicals and reagents

Salts were obtained from Sigma–Aldritch (St. Louis, MO, USA) or Acros (New Jersey, USA) and were of the highest grade available and used as supplied by the manufacturer. The sources of other compounds are as indicated in the text.

Abbreviations: PLA$_2$, phospholipase A_2; hsPLA$_2$GIIA, the secreted group IIA human PLA$_2$; MD, molecular dynamics; ITC, isothermal titration calorimetry; PE, intermolecular potential energy; IRS, interfacial Recognition Site of the Group I/II PLA$_2$s.

* Corresponding author. Fax: +55 (0)16 36024838.
E-mail addresses: rjward@ffclrp.usp.br, rjward@fmrp.usp.br (R.J. Ward).

0045-2068/$ - see front matter © 2009 Elsevier Inc. All rights reserved.
doi:10.1016/j.bioorg.2009.01.002

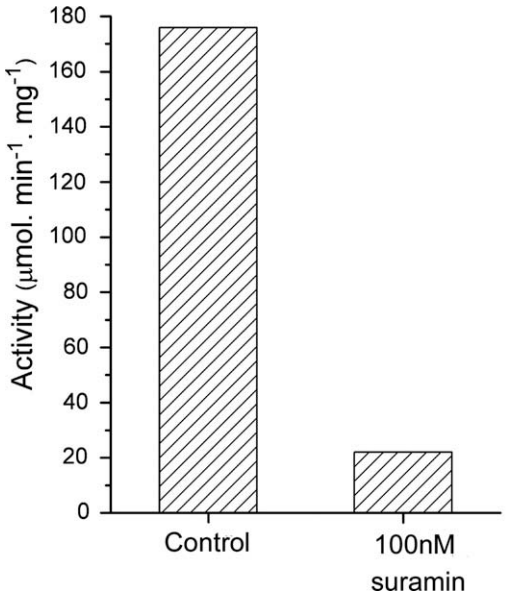

Fig. 1. Inhibition of the catalytic activity of the hsPLA$_2$GIIA by suramin. See Section 2 for further experimental details.

2.2. Recombinant hsPLA$_2$GIIA

A full-length cDNA encoding hsPLA$_2$GIIA (GenBank accession no. BC005919) in vector pDNR-lib was obtained from the I.M.A.G.E Consortium/LNNL (http://image.llnl.gov/, clone ID 4274550). The protein-coding region (CDR) was amplified using oligonucleotides that introduced restriction sites for *Nde*I and *Bam*HI a the 5′ and 3′ extremes of the CDR, and also introduced the mutation N1A, which increases the efficiency of post-translation N-terminal methionine cleavage, without altering in the catalytic properties of the enzyme [16]. The amplified fragment was cloned into the equivalent sites of expression vector pET-3a, and nucleotide sequencing confirmed the expected construct. After expression as inclusion bodies in *Escherichia coli* BL21, the protein was refolding and purified as described previously [13].

2.3. Phospholipase A$_2$ hydrolytic activity assay

The hydrolytic activity of the hsPLA$_2$GIIA was assayed by monitoring fatty acid release via binding to acrylodan conjugated intestinal fatty acid binding protein (ADIFAB – Invitrogen Corp., Carlsbad-CA, USA). Unilamellar liposomes (30 μg/mL) composed of a 1:1 molar ratio of dioleoyl phosphatidylcholine (DOPC – Sigma–Aldrich, St. Louis, MO, USA) and dioleoyl phosphatidylglycerol (DOPG – Sigma–Aldrich, St. Louis, MO, USA) prepared by reverse phase evaporation [17] were mixed with ADIFAB (3 μg/mL) and 0.1 μg mL^{-1} of the enzyme in reaction buffer (20 mM Hepes, 20 mM NaCl, 1 mM $CaCl_2$). For the inhibition experiments, 100 nM suramin (Sigma–Aldrich, St. Louis, MO, USA) was pre-incubated with enzyme for 15 min in the same buffer, and added to the liposome/ADIFAB mixture. The specific activity of the enzyme was determined from the 505 nm/425 nm fluorescence signal ratio measured using a Hitachi 4500 spectrofluorimeter as previously described [18].

2.4. Isothermal titration calorimetry (ITC)

One milliliter of 6 μM hsPLA$_2$GIIA in buffer (NaH_2PO_4; 20 mM, NaCl; 150 mM, pH 7,2) was titrated with a 300 μM of suramin (Sigma–Aldrich, St. Louis, MO, USA), at 25 °C using a Nano-ITC III titration calorimeter (model CSC 5300, Lindon, Utah, USA). The titration experiments consisted of 25 injections, each of 10 μL, with a 300s time delay between the injections. Blank experiments were performed under identical experimental conditions by titration of buffered solution with suramin, and used to correct for dilution, mixing and injection effects. Analyses of the heat flow curves were performed assuming independent binding sites using software provided by the instrument manufacturer.

2.5. Molecular dynamics simulations

The systems for molecular dynamics (MD) simulations were constituted by 16,500 SPC water molecules [19], a monomer of hsPLA$_2$GIIA (PDB code 1POE [20]) and a single suramin molecule. A cubic simulation box was adjusted to give a density of 0.997 kg L^{-3} for the water molecules. The initial suramin localization on the surface of the hsPLA$_2$GIIA was made by superposition of the hsPLA$_2$GIIA with the crystal structure of the complex between suramin and the Lys49-PLA$_2$ from the venom of *Bothrops asper* (PDB code 1Y4L [21]). This procedure located one extremity of the suramin molecule (denominated SUR-1, see Fig. 2A) in the surface cleft that forms the substrate binding/active-site region of the hsPLA$_2$GIIA, and is shown in green in Fig. 2B and 2C. The initial position of the other extremity of the suramin molecule (denominated SUR-2, shown in yellow in Fig. 2B and 2C) and was directed to one of two surface regions rich in arginine and lysine groups located near the N- or the C-terminus of the protein, and the two different conformations were chosen based on electrostatic molecular potential calculations using atoms at the protein surface [22]. After identification of the regions of interest on the protein surface, the two initial conformations were obtained by varying the dihedral angles of the suramin and using an energy minimization process based on the steepest descent method [23].

The conformation in which the SUR-2 makes contact with residues in the N-terminal region was denominated CONF-1, and the conformation in which the SUR-2 is located near the C-terminal region was denominated CONF-2. These two conformations were simulated separately, and in both simulations the initial velocities were obtained from a Maxwell distribution at 298 K. Molecular dynamics simulations were carried out using the GROMACS 3.3.1 software package and the GROMOS-96 (43a2) force field [24]. The charges and topology of suramin were obtained from the Dundee PRODRG Server (http://davapc1.bioch.dundee.ac.uk/cgi-bin/prodrg_beta). All simulations were performed in constant volume, ensemble NVT, using the "leapfrog" algorithm [25] with a time step of 2.0 fs over a total time of 4.0 ns. Temperature was controlled using the Berendsen method [26] with coupling time constants of 0.1 ps. A total of 9 Cl^- counter-ions were included in order to maintain total charge neutrality of the hsPLA$_2$GIIA/suramin complex. Long-range interactions were treated using the particle-mesh Ewald sum (PME) method [27] and calculated with a cutoff of 1.4 nm. The LINCS algorithm [28] was used to constrain the covalent and hydrogen bonds in the protein, and the SETTLE algorithm [29] was used to constrain the geometry of the water molecules.

3. Results and discussion

All Group II PLA$_2$s show a highly conserved interface recognition site (IRS) [30] that defines the surface of the protein that makes contact with the phospholipid membrane. The IRS is comprised of a hydrophobic phospholipid binding cleft surrounded by a ring of polar residues. In the hsPLA$_2$GIIA, residues located in the C-terminal loop contribute to the IRS, and charge-reversal mutagenesis of cationic residues in this region reduces the catalytic activity, suggesting that electrostatic interactions with negatively charged

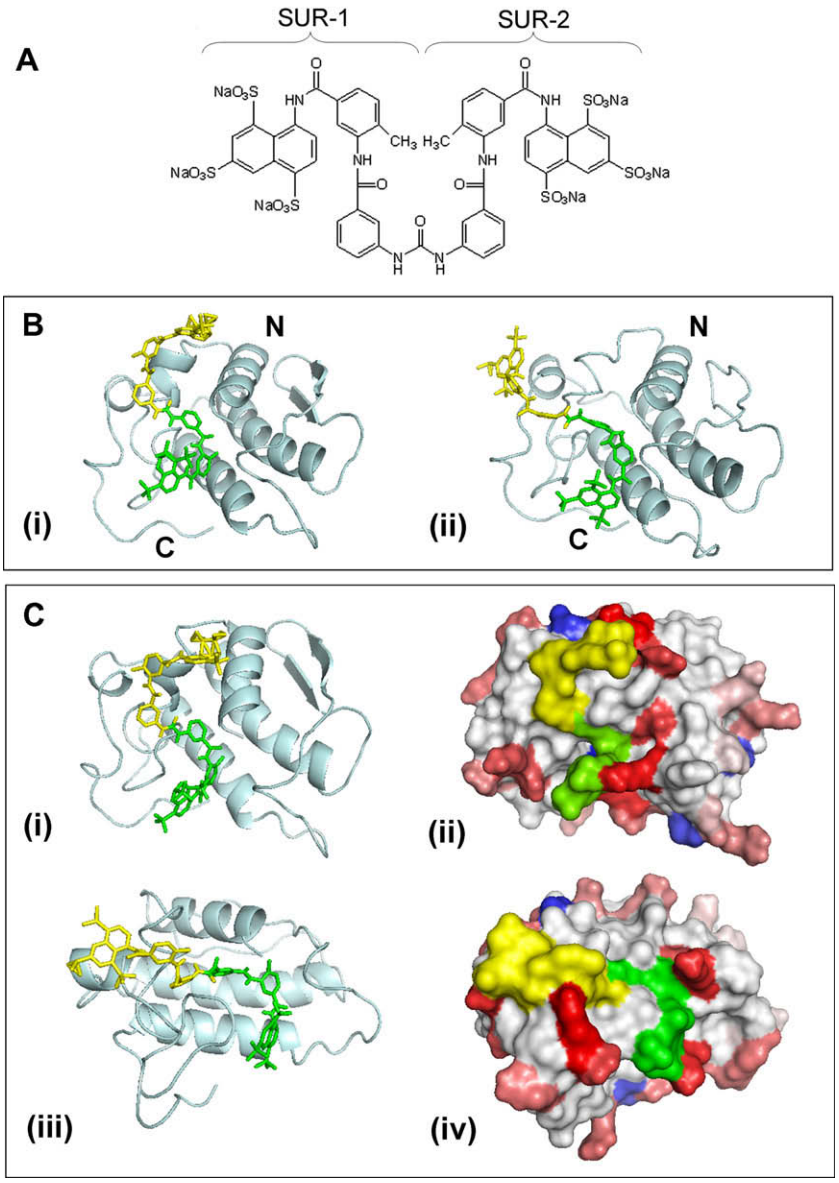

Fig. 2. (A) Chemical structure of suramin showing the division of the molecule (regions denoted as SUR-1 and SUR-2) for analysis of the molecular simulation data. (B) Ribbon representations of the hsPLA$_2$GIIA/suramin complex looking towards the interfacial recognition surface (IRS) of the protein. The stick model of the bound suramin is coloured according to the SUR-1 (green) and SUR-2 (yellow) regions. The two suramin conformations CONF-1 (i) and CONF-2 (ii) are shown, in which the SUR-2 makes contacts with amino-acids around the N- and C-terminal regions of the protein, respectively (indicated as N and C). (C) Ribbon and solid surface representations of the CONF-1 (Figs. 1 and 2) and CONF-2 (Figs. 3 and 4) conformations of the hsPLA$_2$GIIA/suramin complexes. The ribbon representations (i) and (iii) show the orientations of the complex for the solid surface representations in Figs. 2 and 4, in which the SUR1 and SUR-2 regions of the suramin molecules are shown in green and yellow, respectively. The solid surface representations are coloured according to the sum of the potential energy of all atoms in each residue calculated from the results of molecular dynamics simulation, with increasingly intense shades of red for a negative (attractive) potential, and blue for a positive (repulsive) potential.

membrane phospholipids mediate the contact of this loop with the membrane [31,32]. Furthermore, residues in the N-terminal region of the hsPLA$_2$GIIA also contribute to the IRS of the protein [31,32], therefore all the regions identified as suramin binding sites in the MD study are likely to influence the interaction of the protein with the phospholipid membrane. The interaction of suramin with the hsPLA$_2$GIIA might therefore interfere not only with the interaction of the protein with the membrane, but also could directly compete with substrate access to the active-site. The inhibitory effect of suramin on phospholipid hydrolysis by the hsPLA$_2$GIIA was demonstrated by measuring the reduction of free fatty release using a mixed phospholipid substrate (Fig. 1). The specific catalytic activity of the enzyme against liposome membranes containing DOPC/DOPG was 176 μmol min^{-1} mg^{-1} (control in Fig. 2), which is similar to the activity previously reported using this lipid mixture [13,33]. The addition of suramin at a concentration of 100 nM inhibits approximately 90% of the PLA$_2$ hydrolytic activity.

Initial localization of the suramin on the surface of the hsPLA$_2$GIIA identified two alternative conformations (denominated CONF-1 and CONF-2 – see Section 2). As shown in Fig. 2, the SUR-2 region of the suramin in CONF-1 is oriented the N-terminus of the protein (Fig. 2B(i)), and that in CONF-2 the SUR-2 region of the suramin is oriented towards the C-terminal loop (Fig. 2B(ii)). The regions around the N-terminal helix and C-terminal loop are rich in positively charged residues, and therefore satisfy the key criterion for potential binding sites for the polyanionic suramin. MD simulations were used to evaluate in more detail the regions of the protein which may be involved in the suramin/hsPLA$_2$GIIA complex formation. The

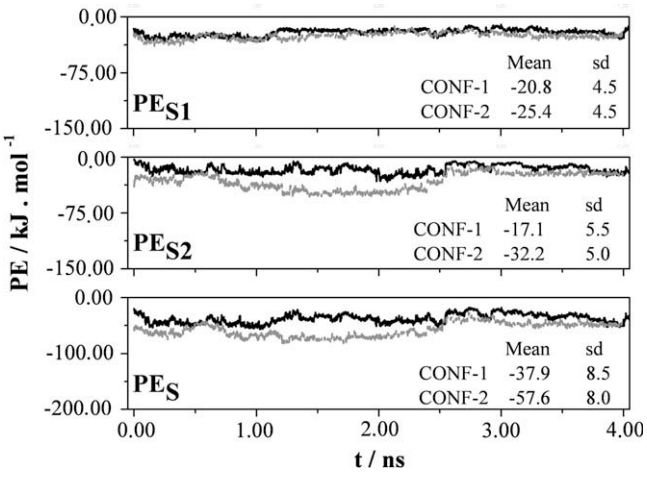

Fig. 3. Trajectories of the potential energy (PE) for the hsPLA$_2$GIIA/suramin complexes. The mean values for the PE values of both the CONF-1 and CONF-2 conformations are shown for the SUR-1 and SUR-2 regions of the suramin (upper and middle panels, PE_{S2} and PE_{S1}, respectively), and the complete suramin molecule (lower panel – PE_S).

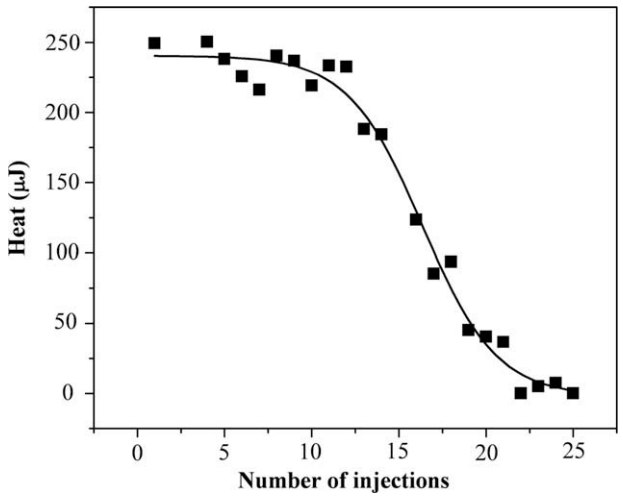

Fig. 4. Calorimetric curve of the interaction between the suramin with the hsPLA$_2$GIIA obtained by isothermal titration calorimetry (ITC). The solid line represents the best fit to the experimental data using an independent binding model (see Section 2 for further details).

calculated potential energy (PE) is the sum of electrostatic and Lennard–Jones potentials resulting from the interaction of non-bonded atoms, and is a useful parameter for evaluating putative binding sites in the complex. Fig. 2C shows solid surface representations of both suramin/hsPLA$_2$GIIA conformations, in which each residue has been coloured in accord with its attractive (red) or repulsive (blue) contribution to the overall intermolecular PE. In both conformations, residues surrounding the contact regions between suramin and the protein are rich in cationic residues that make strong negative contributions to the intermolecular PE.

The total intermolecular potential energy is the sum of the interactions between hsPLA$_2$GIIA and the SUR-1 and SUR-2 regions of the suramin. These potential energies were designated as PE_{S1} (PE between hsPLA$_2$GIIA and SUR-1), PE_{S2} (PE between hsPLA$_2$GIIA and SUR-2) and PE_S (the total PE between hsPLA$_2$GIIA and suramin, equal to the sum of PE_{S1} and PE_{S2}). The trajectories of these potential energies are presented in Fig. 3, which shows that the potential energy profiles of PE_{S1} (Fig. 3, upper panel) are similar for CONF-1 and CONF-2, with highly attractive energies varying between -10.0 and -34.0 kJ mol^{-1}. In contrast, the PE_{S2} trajectories of the SUR-2 region of the suramin in the CONF-1 and CONF-2 conformations present different profiles (Fig. 3, middle panel). Although a lower mean energy was attained during the simulation of the CONF-2 conformation, at the end of time-course the energies of both conformations were approximately equal. The average taken over the entire simulation suggests that the CONF-2 is favored by a PE energy difference of -15.0 kJ mol^{-1}. Furthermore, the standard deviations of the PE are reduced in the CONF-2 simulation in comparison with CONF-1, which is characteristic of a more stable conformation. The observed differences in the total PE (PE_S) during the simulation (Fig. 3, lower panel) reflect the different interactions of the SUR-2 region of the suramin with the protein in the CONF-I and CONF-2 conformations.

The MD studies identified three regions that may be involved in the formation of the suramin/hsPLA$_2$GIIA complex, and this prediction was evaluated by isothermal titration calorimetry (ITC). Results of the ITC of hsPLA$_2$GIIA with suramin are presented in Fig. 4, and fitting of the calorimetric titration curve was best described by an independent binding model that identified 2.7 suramin binding sites per protein molecule, which is consistent with the number of sites predicted by the MD simulations. The observed enthalpy of interaction of suramin injected is endothermic with a value of 119.8 kJ mol^{-1} and the apparent binding affinity of the suramin to the hsPLA$_2$GIIA was 4.2×10^{-6}.

In summary, the results of ITC experiments suggest that the hsPLA2GIIA presents three suramin binding sites, and an analysis of the electrostatic characteristics of the two molecules involved in complex formation, it was possible to predict two conformations of the bound suramin based on the charged group interactions by MD technique. These results predict that the three suramin binding sites in the hsPLA$_2$GIIA observed in the ITC experiments are located in (1) the substrate binding/active-site region, (2) in the region surrounding residues in the N-terminal region, and (3) in the region surrounding residues in the C-terminal region of the protein. These results provide predictions that may be further tested by evaluating the interaction of suramin with site-directed mutants of the hsPLA$_2$GIIA.

Acknowledgments

The financial support of CNPq (Grant Nos. 304982/2006-7 [RJW], 152669/2007-8 [DSV]), FAPESP (Grant No. 05/50379-0 [EAA]) and PRP-USP is acknowledged.

Appendix A. Supplementary material

Supplementary data associated with this article can be found, in the online version, at doi:10.1016/j.bioorg.2009.01.002.

References

[1] L.L.M. van Deenen, G.H. de Haas, Biochem. Biophys. Acta 70 (1963) 538–553.
[2] R.H. Schaloske, E.A. Dennis, Biochim. Biophys. Acta 1761 (11) (2006) 1246–1259.
[3] P. Vadas, J. Browning, J. Edelson, W. Pruzanski, J. Lipid Mediat. 8 (1) (1993) 1–30.
[4] X.D. Qu, R.I. Lehrer, Infect Immunol. 66 (6) (1998) 2791–2797.
[5] S.S. Harwig, L. Tan, X.D. Qu, Y. Cho, P.B. Eisenhauer, R.I. Lehrer, J. Clin. Invest. 95 (2) (1995) 603–610.
[6] M. Murakami, Y. Nakatani, G. Atsumi, K. Inoue, I. Kudo, Crit. Rev. Immunol. 17 (3–4) (1997) 225–283.
[7] A.G. Buckland, E.L. Heeley, D.C. Wilton, Biochim. Biophys. Acta 1484 (2–3) (2000) 195–206.
[8] V.J. Laine, D.S. Grass, T.J. Nevalainen, J. Immunol. 162 (12) (1999) 7402–7408.
[9] A. Den Hertog, J. Van den Akker, A. Nelemans, Eur. J. Pharmacol. 173 (2-3) (1989) 207–209.
[10] M. Freissmuth, M. Waldhoer, E. Bofill-Cardona, C. Nanoff, Trends Pharmacol. Sci. 20 (6) (1999) 237–245.
[11] S.Y. Lin-Shiau, M.J. Lin, Eur. J. Pharmacol. 382 (2) (1999) 75–80.

[12] M. de Oliveira, W.L. Cavalcante, E.Z. Arruda, P.A. Melo, M. Dal-Pai Silva, M. Gallacci. Toxicon 42 (4) (2003) 373–379.
[13] E.A. Aragão, L. Chioato, T.L. Ferreira, A.I. De Medeiros, A. Secatto, L.H. Faccioli, R.J. Ward, Inflamm. Res. 58 (2009) 1–8.
[14] V. Magrioti, G. Kokotos, Anti-Inflamm. Anti-Allergy Agents Med. Chem. 5 (2006) 189–203.
[15] R.C. Reid, Curr. Med. Chem. 12 (25) (2005) 3011–3026.
[16] R. Othman, S. Baker, Y. Li, A.F. Worrall, D.C. Wilton, Biochim. Biophys. Acta 1303 (2) (1996) 92–102.
[17] T.L. Ferreira, R. Ruller, L. Chioato, R.J. Ward, Biochimie 90 (9) (2008) 1397–1406.
[18] G.V. Richieri, A.M. Kleinfeld, Anal. Biochem. 229 (2) (1995) 256–263.
[19] H.J.C. Berendsen, J.P.M. Postma, W.F. van Gunsteren, J. Hermans, Interactions Models for Water in Relation to Protein Hydration, Reidel Publishing Company, Dordrecht, 1981.
[20] D.L. Scott, S.P. White, J.L. Browning, J.J. Rosa, M.H. Gelb, P.B. Sigler, Science 254 (5034) (1991) 1007–1010.
[21] M.T. Murakami, E.Z. Arruda, P.A. Melo, A.B. Martinez, S. Calil-Elias, M.A. Tomaz, B. Lomonte, J.M. Gutierrez, R.K. Arni, J. Mol. Biol. 350 (3) (2005) 416–426.
[22] P.K. Weiner, R. Langridge, J.M. Blaney, R. Schaefer, P.A. Kollman, Proc. Natl. Acad. Sci. USA. 79 (12) (1982) 3754–3758.
[23] G. Arfken, The Method of Steepest Descents in Mathematical Methods for Physicists, third ed., Academic Press, Orlando, 1985.
[24] E. Lindahl, B. Hess, D. van der Spoel, J. Mol. Mod. 7 (2001) 306–317.
[25] R.W. Hockney, S.P. Goel, J. Comp. Phys. 14 (1974) 148–158.
[26] H.J.C. Berendsen, J.P.M. Postma, A. DiNola, J.R. Haak, J. Chem. Phys. 81 (1984) 3684–3690.
[27] T. Darden, D. York, L. Pedersen, J. Chem. Phys. 98 (1993) 10089–10092.
[28] B. Hess, H. Becker, H.J. Berendsen, J.G.E.M. Fraaije, J. Comp. Chem. 18 (1997) 1463–1472.
[29] S. Miyamoto, P.A. Kollman, J. Comp. Chem. 13 (1992) 952–962.
[30] W.A. Pieterson, J.C. Vidal, J.J. Volwerk, G.H. de Haas, Biochemistry 13 (7) (1974) 1455–1460.
[31] S.A. Beers, A.G. Buckland, R.S. Koduri, W. Cho, M.H. Gelb, D.C. Wilton, J. Biol. Chem. 277 (3) (2002) 1788–1793.
[32] R.S. Koduri, J.O. Gronroos, V.J. Laine, C. Le Calvez, G. Lambeau, T.J. Nevalainen, M.H. Gelb, J. Biol. Chem. 277 (8) (2002) 5849–5857.
[33] A.G. Singer, F. Ghomashchi, C. Le Calvez, J. Bollinger, S. Bezzine, M. Rouault, M. Sadilek, E. Nguyen, M. Lazdunski, G. Lambeau, M.H. Gelb, J. Biol. Chem. 277 (50) (2002) 48535–48549.